Microscopic optical potential for low energy α-particles interacting with A$\sim$ 100 target nuclei *

M. Avrigeanu[1], W. von Oertzen[2], A.J.M. Plompen[3], and V. Avrigeanu[1]

[1] *"Horia Hulubei" National Institute for Physics and Nuclear Engineering, P.O. Box MG-6, 76900 Bucharest, Romania*

[2] *Freie Universität Berlin, Fachbereich Physik, Arnimallee 14, 14195 Berlin, and Hahn-Meitner-Institut, Glienicker Strasse 100, 14109 Berlin, Germany*

[3] *European Commission, Joint Research Centre, Institute for Reference Materials and Measurements, Retieseweg, B-2440 Geel, Belgium*

A semi-microscopic analysis based on the Double Folding (DF) model for the α-particle elastic scattering on A$\sim$100 nuclei at energies below 32 MeV has been carried out. The energy-dependent phenomenological imaginary part for this semi-microscopic optical model potential was obtained, making use also of the dispersive correction to the microscopic real potential. This imaginary potential has then been introduced within a complete phenomenological analysis of the same data basis. A regional parameter set of the phenomenological OMP for low-energy α-particles has thus been obtained for nuclei in the mass range A$\sim$100, which is of interest to basic nuclear physics as well as nuclear technology.

I. INTRODUCTION

Priority of actual nuclear reaction data requirements at medium energies should be given to a better description of the ground-state properties and the α-particle optical potential [1]. The nuclear data for α-particle emission for the isotopes of Zr and Mo are among the high-priority requests for nuclear astrophysics applications as well as for the accurate account of the important effects of α-particle interactions in the nuclear engineering design of the fusion test facilities and accelerator-driven systems, namely the radiation-damage, activation, heating, and shielding requirements.

The α-particle optical model potential (OMP) is essential for the understanding of α-particle elastic scattering, and calculations of α-induced reaction cross sections as well as α-particle emission from compound reactions. However, unlike in the nucleon case, there are no global potentials for α-particles that fit to good accuracy the scattering from many nuclei over a wide range of energies (e.g., the IAEA Reference Input Parameter Library [2]). Moreover, results from the analysis of the low-energy elastic scattering data suffer from discrete and continuous ambiguities in the OMP parameters, whose uncertainties vary for various target nuclei and for different incident energies due to the precision of the data analysed. Therefore, in order to avoid too much phenomenology in the description of these data, numerous attempts have been made to replace the phenomenological real potential of Woods-Saxon (WS) type by a more microscopic α-nucleus potential using an effective interaction.

In addition to the recent result of Khoa [3] the present work looks for suitable constraints for OMP parameters at α-particle energies around the Coulomb barrier, taking also into account the latest studies [4,5]. Thus, in Sec. II we have first considered a semi-microscopic OMP with a DF real part, but using the most advanced version with the explicit treatment of the exchange component [3,6] and no adjustable parameter or normalization constant. The semi-microscopic analysis of the experimental α-particle elastic scattering on A$\sim$100 nuclei at energies below 32 MeV, performed in order to adopt a proper energy-dependent phenomenological imaginary part is presented in Sec. III. The study is completed in Sec. IV by a full phenomenological analysis of the same data.

II. THE DOUBLE FOLDING POTENTIAL

The direct and exchange real parts of the microscopic optical potential are usually given in terms of the projectile and the target nuclear densities $\rho_1(\mathbf{r}_1)$ and $\rho_2(\mathbf{r}_2)$ respectively, which are folded with the density- and energy-dependent effective NN interaction $v(\rho, E, \mathbf{s}{=}\mathbf{R}{+}\mathbf{r}_2{-}\mathbf{r}_1)$. Since the details of the folding procedure are given elswhere [7–9], only ths basic points are resumed in the following.

*Contributed paper to the 10th International Conference on Nuclear Reaction Mechanisms, Varenna, June 9-13, 2003

In the semi-microscopic double folding model of Khoa *et al.* [8] the NN-interaction is introduced with a density dependence, which is modelled to reproduce within a corresponding Hartree-Fock calculation the saturation properties of nuclear matter. [7,8]. This dependence accounts for the reduction in the strength of the interaction that occurs as the density of the surrounding medium increases, and has been essential to explain the nuclear rainbows seen in α-particle scattering at high energies. The density-dependent DDM3Y and BDM3Y effective NN interactions have been obtained by multiplying with the density-dependent function $F(\rho)$ [8] with 2 or 3 parameters adjusted by reproducing the saturation point of nuclear matter and a compressibility modulus of $K \approx 230$ MeV:

$$F(\rho) = \begin{cases} C[1+\alpha\exp(-\beta\rho)], & \text{for DDM3Y} \\ C(1-\alpha\rho), & \text{for BDM3Y ,} \end{cases} \tag{1}$$

where C=0.2963, α=3.7231, and β=3.7384 for the DDM3Y type, while C=1.2521 and α=1.7452 for the BDM3Y type. The density dependent factors were chosen to reproduce the same saturation point of nuclear matter, but different compressibilities K. If K is fixed the resulting real potentials do not depend anymore on the NN interaction chosen.

In addition to the density dependence [8] a small energy dependence is introduced, with an energy-dependent factor which is a linear function of the incident energy per nucleon E of the form $g(E)$=1-γE. The coefficient γ has the values 0.002 and 0.003 for the M3Y-Reid [10] and M3Y-Paris [11] interactions, respectively.

There is a particular case of α-particle scattering, namely the α-α system where the potential is real for incident energies below the reaction threshold of 34.7 MeV for the first open channel ^{7}Li + p. It is thus possible to make a check of the DF real potential independent from the imaginary potential which is quite useful for further works involving the α-particle. The analysis of this case may therefore provide unambiguous information on the choice of effective NN interactions as well as of the α-particle density distributions. Therefore we have found [6] that the best description of these data [12–14] is obtained by using the Reid effective NN interaction folded with Baye *et al.* [15] α-particle density distribution.

The nuclear density distribution of the target nuclei has been described by means of a Fermi-type distribution with the parameters based on the electron scattering data [16,17] and shell model calculations [18]. Thus, the parameterization of Negele [16] has been used for ^{91}Zr, ^{92,94,96,98,100}Mo, ^{107}Ag, and ^{122,124}Sn, while the parameterizations of Farid and Satchler [18] and Lightbody *et al.* [17] have been used for the density distribution of ^{90}Zr and ^{116}Sn, respectively.

III. THE SEMI-MICROSCOPIC OPTICAL POTENTIAL ANALYSIS

In the present work we have looked for a consistent OMP able to describe the bulk of α-particle elastic scattering data on A$\sim$100 target nuclei at low incident energies ($\leq$32 MeV) [4,19–22]. According to the discussions in previous section we use the semi-microscopic DF real potential based on the α-particle density distribution of Baye *et al.* [15] and the BDM3Y Reid effective NN-interaction, Eq. (1), and the phenomenological mass- and energy-dependent imaginary potential. The scattering cross sections were calculated by using the computer code SCAT2 [23], modified to include the semi-microscopic DF potential as an option for the OMP real part.

The starting point in choosing the imaginary component of the potential has been the global OMP developed for energies above 80 MeV [24] and extensively applied for low-energy alpha-particles [25] emitted from compound nuclei. Its further extension to lower energies for the processes in the incident channel, proved to be more complex due to the interplay of the contributions of the barrier and internal waves [26], has been the goal of the present work.

Within our two-step OMP approach, we determined first the parameters of the imaginary part with a "parameter free" DF-real potential able to describe the experimental angular distributions of α-particle elastic-scattering on target nuclei from ^{89}Y to ^{124}Sn and α-particle energies from 13 to 32 MeV. In the next step a phenomenological real part has been chosen within the general form of the optical potential with Woods-Saxon form factors for the real and imaginary parts

$$U(r) = V_c(r) + V_R\, f(r,R_R,a_R) \;+\; iW_V\; f(r,R_V,a_V) \;+ iW_D\, g(r,R_D,a_D) \tag{2}$$

where $f(r,R_i,a_i)$=(1+exp[(r-R_i)/a_i])$^{-1}$, $g(r,R_i,a_i)$=-4a_id/dr[$f(r,R_i,a_i)$], and R_i=r_i $A^{1/3}$, A being the target-nucleus mass number. $V_c(r)$ is a Coulomb potential of a uniformly charged sphere of radius R_c, while r_c= 1.30 fm.

For the imaginary part, an additional surface term with the derivative shape is introduced because of the importance of direct reactions. The surface term is mainly needed at smaller energies, where the number of direct channels is still small. Thus the surface term has been chosen so that it decreases with increasing energy and vanishes at 28 MeV.

It should be emphasized that no adjustable parameter or normalization constant has been involved for the DF real part in order to couple the imaginary part of the OMP so that the predictive power of this semi-microscopic potential is preserved. Actually the widely used renormalization factor N_R [3] for the real semi-microscopic potential is a convenient way to take into account the absorption from the elastic channel and the presence of couplings to other channels [27,28]. On the other hand, these effects can be represented by the real "dynamical polarization potential" which can be described [29–31] by a dispersive contribution added to the total real potential. We have used the analytical solution given by Eqs. (3.13)-(3.16) of Ref. [29] for the dispersion relation. In this solution a linear schematic model has been used, with the reference energy E_S=25 MeV. Moreover, dispersive correction is obtained by contributions of the corresponding volume and surface components (see Ref. [6] for more details).

The effect of dispersion correction in the analysis is shown in Figs. 1 and 2, leading to a better agreement between the calculated elastic-scattering cross sections and the experimental data. The most suggestive results in this respect are obtained for the isotopes ^{89}Y, ^{90,91}Zr, and ^{92}Mo. The imaginary potential well depths obtained by the fit of the data are shown in Table 1 while the corresponding potential geometry parameters are given by Eqs. (3-6) in the next section.

Table 1. Optical potential parameters and volume integrals, obtained by fits of the α-particle elastic-scattering data for A$\sim$100 nuclei at low energies. The rest of the parameter sets are defined in Eqs. (3) - (6).

Target Nucleus	E_α (MeV)	V_R (MeV)	a_R (fm)	W_V (MeV)	W_D (MeV)	J_R^{DF} (MeV·fm^3)	J_R^{ph} (MeV·fm^3)	J_V (MeV·fm^3)	J_D (MeV·fm^3)
^{89}Y	21.0	150	0.653	6.5	7.8	292	372	28.4	20.4
	23.4	148	0.655	8.5	3.7	288	368	37.1	9.7
	25.0	149	0.656	10.0	2.5	283	370	43.7	6.6
^{90}Zr	15.0	165	0.630	7.5	0.0	300	406	32.7	0.0
	21.0	150	0.655	6.5	6.7	294	372	28.4	17.4
	23.4	149	0.656	8.0	4.3	290	370	34.9	11.2
	25.0	148	0.662	9.0	3.0	286	368	39.3	7.8
^{91}Zr	21.0	150	0.657	6.7	6.9	291	372	29.2	17.8
	23.0	148	0.659	8.0	5.2	288	368	34.9	13.4
	25.0	148	0.660	10.0	3.5	283	368	43.6	9.0
^{92}Mo	13.84	161	0.633	7.5	1.5	297	396	32.7	3.9
	16.42	155	0.640	7.0	4.0	296	382	30.5	10.3
	19.5	150	0.652	7.5	6.9	293	371	32.7	17.7
	32.2	157	0.659	12.0	0.0	281	390	52.3	0.0
^{94}Mo	25.2	155	0.666	14.0	3.0	282	384	61.0	7.6
	32.2	157	0.665	12.0	0.0	280	390	52.3	0.0
^{96}Mo	32.2	157	0.671	11.0	0.0	280	390	47.9	0.0
^{98}Mo	32.2	158	0.676	13.0	0.0	279	393	56.5	0.0
^{100}Mo	32.2	157	0.681	10.0	0.0	279	390	43.4	0.0
^{107}Ag	15.0	166	0.638	6.5	0.0	294	405	28.1	0.0
	25.2	153	0.659	10.5	2.0	281	376	45.4	4.7
^{116}Sn	25.2	163	0.669	13.8	2.8	292	399	59.5	6.2
^{122}Sn	25.2	150	0.670	10.5	1.0	278	366	45.1	2.1
^{124}Sn	25.2	152	0.672	10.0	2.0	285	371	43.0	4.2

Table 2. Parameters to obtain the well depth and diffuseness [Eqs. (3) - (6)] for the regional OMP (see text).

a_0 (MeV)	102.8 $\pm$ 22.8
a_1 (MeV)	5.18 $\pm$ 2.46
a_2	-0.14 $\pm$ 0.21
b_0 (MeV)	1.98 $\pm$ 1.49
b_1	0.31 $\pm$ 0.06
c_0 (fm)	0.505 $\pm$ 0.072
c_1 (fm)	0.033 $\pm$ 0.016

Particular comments are needed for the description of the behaviour of angular distributions at 23 MeV observed by Wit *et al.* [20]. The experimental excitation functions (E_α=18-25 MeV) and angular distributions ($\theta_{c.m.} \sim 50^o$-180^o) of the α-particle elastic scattering on ^{89}Y and ^{90,91}Zr [20] show a drop of the cross-section around E_α=23 MeV, correlated with a deep minimum close to 180^o in the angular distributions at that energy. While a maximum is observed at this angle for the majority of experimental α-particle elastic-scattering angular distributions, this maximum was also found by Wit *et al.* at the neighboring energies of 21 and 25 MeV. Recently it was shown by Michel *et al.* [32] that incomplete absorption, which so far has been observed for α-particle scattering from light nuclei at low energies [33,34], persists in fact at least up to ^{90}Zr, and the interesting minimum around 180^o is the result of interference between the internal and barrier wave contributions to the scattering amplitude at this angle and energy. Therefore the appropriate description of this particular behavior by the present OMP proves the correct account of the nuclear absorption.

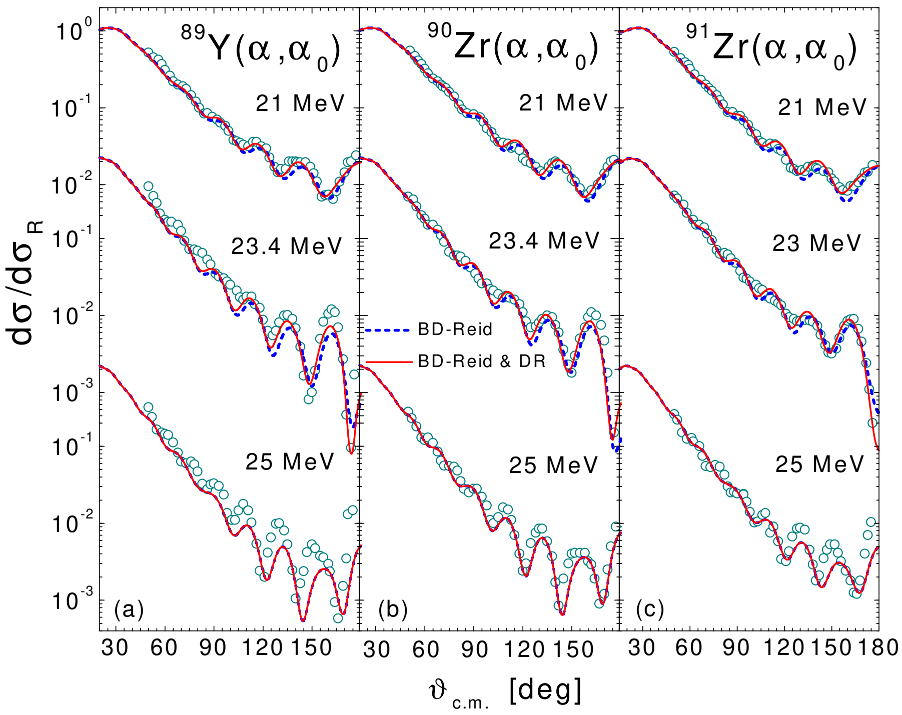

FIG. 1. Comparison of the experimental angular distributions of the elastic scattering of α-particles on (a) ^{89}Y, (b) ^{90}Zr, and (c) ^{91}Zr at 21, 23.4 and 25 MeV [20], with OMP calculations based on the semi-microscopic DF approach without (dotted curves) or including (solid curves) the dispersion correction (DR) respectively

.

Concerning the option on the density-dependence form of the effective NN interaction (1), we have analysed in Fig. 3 the microscopic angular distributions of the elastic-scattered α-particles on ^{90}Zr, calculated by using the M3Y-, DDM3Y- and BDM3Y-Reid interactions [8]. The best description of the experimental data [20] has been found for the density-dependence of the effective NN interaction in the linear, i.e. of the BDM3Y, form. The differences between angular distributions obtained with the pure M3Y and those corresponding to the BDM3Y interaction respectively, are also less pronounced at these energies than those between the BDM3Y and DDM3Y interactions, the latter corresponding to the exponential density dependence of the effective NN interaction which does not reproduce saturation point of nuclear matter [8].

IV. PARAMETERS FOR REGIONAL OPTICAL POTENTIAL AROUND THE COULOMB BARRIER

While only the imaginary potential parameters have been fixed within the semi-microscopic analysis described in Sec. III, the second step is concerned with the determination of a phenomenological real part of the OMP and the use of the already determined imaginary part. The advantage of having well settled already at least half of the usual OMP parameters increases obviously the accuracy of fitting the data. As can be seen in Figs. 4 and 5 even a better description is obtained in comparison with the microscopic analysis. The well depth and diffuseness values of the real potential of Woods-Saxon shape are given also in Table 1 together with the imaginary potential depths unchanged from the first step of the data analysis.

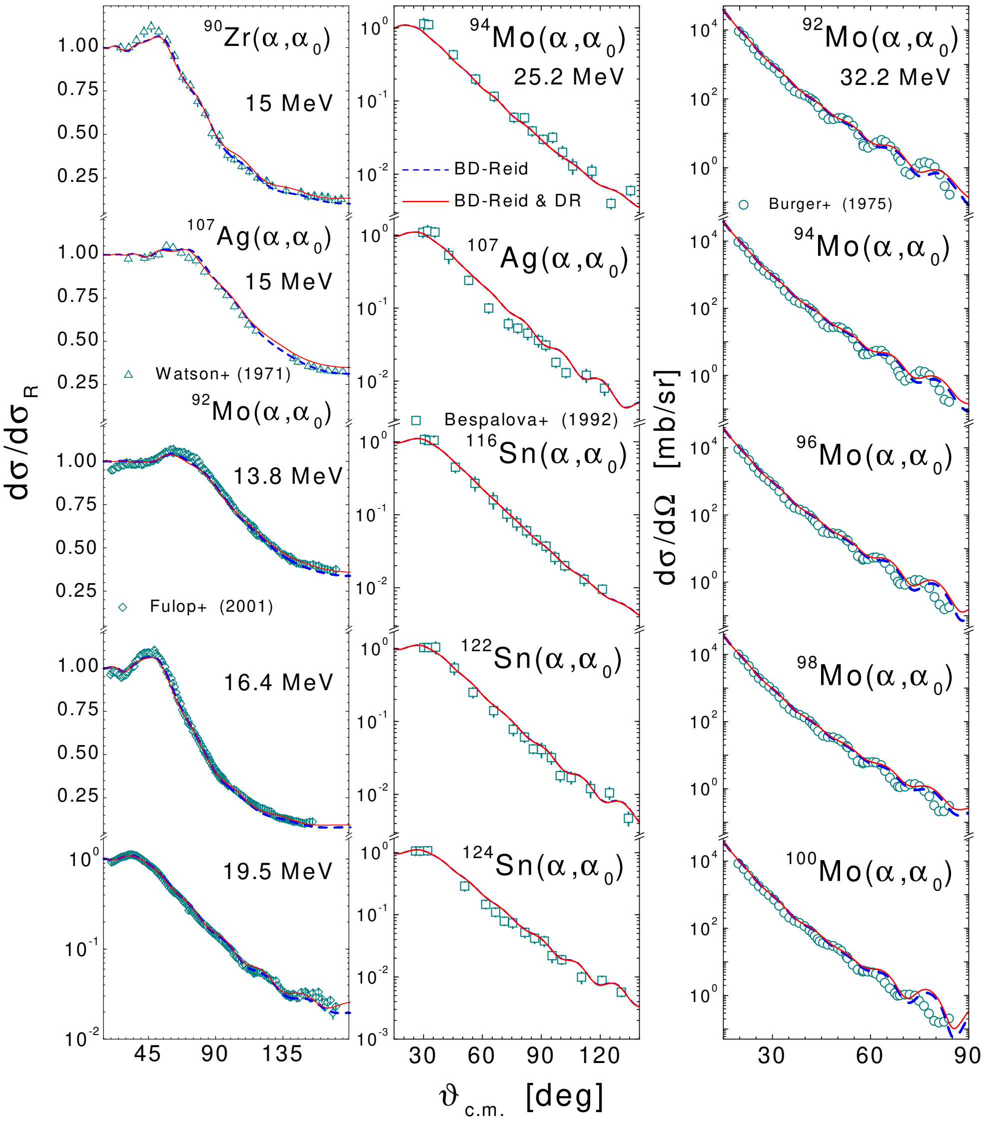

FIG. 2. The same as in Fig. 1 but for α-particle scattered at 15 MeV on ^{90}Zr and ^{107}Ag [19], at 13.85, 16.42, and 19.5 MeV on ^{92}Mo [4], at 25.2 MeV on ^{94}Mo, ^{107}Ag, and ^{116,122,124}Sn [21], and at 32.2 MeV on ^{92,94,96,98,100}Mo [22].

The corresponding expressions for the average mass-, charge-, and energy-dependent well depths (similar to those from Refs. [24,25]) as well as the geometry parameters of the potential given in Eq. (2) are now as follows:

$$V_R = a_0 + a_1\, Z/A^{1/3} + a_2\, E_\alpha, \quad r_R = 1.281, \quad a_R = c_0 + c_1\, A^{1/3}\ , \tag{3}$$

$$W_V = b_0 + b_1\, E_\alpha, \quad r_V = 1.57, \quad a_V = 0.724 - 0.022\, A^{1/3}\ , \tag{4}$$

$$W_D = \begin{cases} -6.67 + 0.667\,E_\alpha, & \text{for } 10 \text{ MeV} < E_\alpha \leq 16 \text{ MeV}, \\ 4, & \text{for } 16 \text{ MeV} < E_\alpha \leq 24 \text{ MeV}, \\ 28 - E_\alpha, & \text{for } 24 \text{ MeV} < E_\alpha \leq 28 \text{ MeV} \end{cases} \tag{5}$$

$$r_D = 1.52, \quad a_D = 0.729 - 0.074\,A^{1/3} \ , \tag{6}$$

where the energies are in MeV and geometry parameters in fm. The resulting average well depth and diffuseness parameters are given in Table 2, where the related uncertainties correspond to the linear-fit errors for each set of local parameter values in Table 1 and mark their spread around the average value.

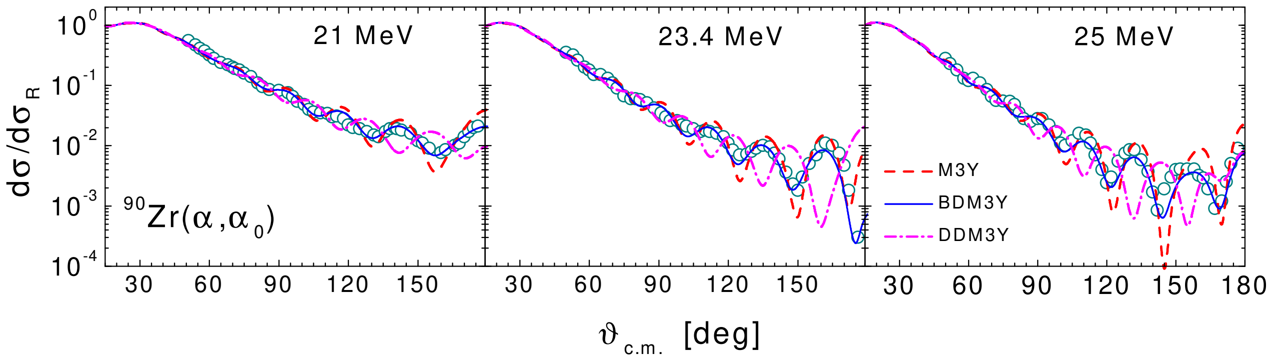

FIG. 3. Comparison of the experimental angular distributions of the elastic scattering of α-particles on ^{90}Zr at 21, 23.4 and 25 MeV [20], with OMP calculations based on the semi-microscopic DF approach obtained by using the α-particle density distribution of Baye *et al.* [15] and the M3Y- (dashed curves), BDM3Y- (solid curves), and DDM3Y-Reid effective NN interactions (dash-dotted curves), including the dispersion correction.

The angular distributions calculated by using these average parameters (regional OMP) as well as the global parameter set of McFadden and Satchler [35] are also shown in Figs. 4 and 5, in order to establish the usefulness of the former OMP and the deviations of its predictions from the local analysis results. One can see thus the present regional potential is able to describe appropriately even nuclear absorption for the particular case of Wit *et al.* data [20] at 23 MeV (Fig. 4).

For the general discussion and for comparison with other work we have also calculated the volume integrals per interacting nucleon pair

$$J_R(E) = \frac{1}{A_1\,A_2} \int U_R(r,E)\,d^3r. \tag{7}$$

The result for the semi-microscopic BDM3Y potential (DF) is also shown in Table 1, together with the values of the real J_R^{ph} and imaginary volume J_V and surface J_D components of the present phenomenological potential. The differences between the semi-microscopic and phenomenological real volume integrals shown in Table 1 come mainly from the different radial dependence of the corresponding potentials [6]. However these potentials are almost identical in the tail region, i.e. for absolute values $\leq$10 MeV and extends over a wider radial range for lower incident energies which may explain the actual similar good description of the elastic scattering data at low energies. On the other hand, their well depths have close and higher central values which is important for the inner turning point contributions needed to describe the large angle scattering (see Figs. 1 and 4). Actually the present semi-microscopic volume-integrals are within around 10 % higher than the DF values which are usually obtained when the normalization constant λ and scaling factor w have been taken 1 [4,36], and around 10 % lower than the corresponding final values after normalization. At the same time our values are similar to those obtained by means of the semi-microscopic potential III of [5] at the same energies, as well as those derived from the analysis of α decay [37]. On the other hand, the present volume integrals for the real phenomenological potential for ^{90}Zr are in agreement within also 10 % with recent values reported by Michel *et al.* [32].

An obviously improved agreement of the calculated and experimental angular distributions is observed at the incident energy of 32 MeV (right hand side Fig. 5) on Mo isotopes.

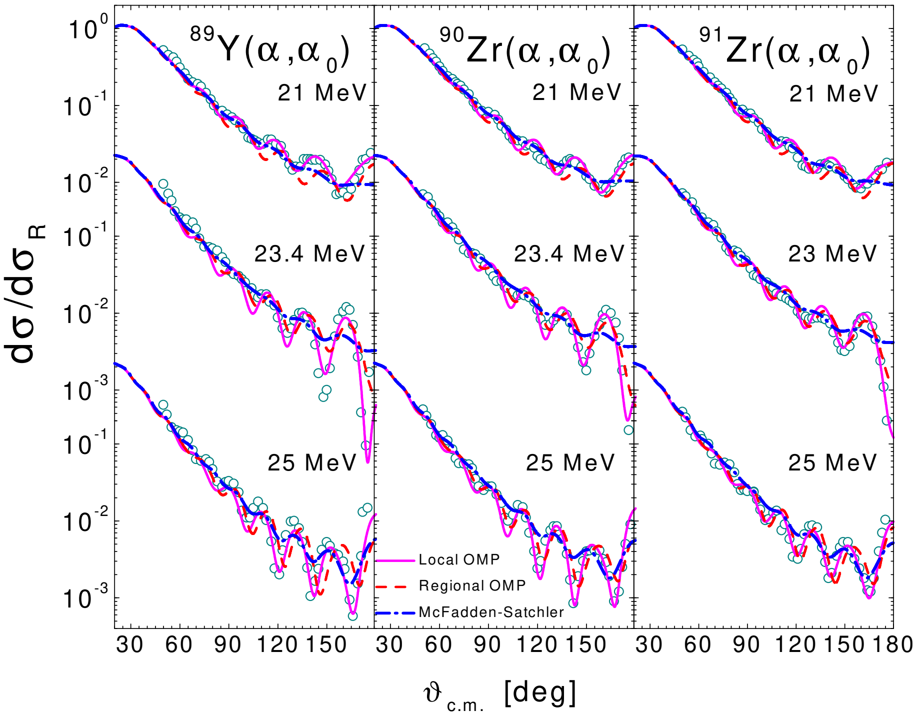

FIG. 4. The same as in Fig. 1 by using the phenomenological OMP parameters of Eqs. (5.1) and either Table 1 (solid curves) or Table 2 (i.e. the regional parameter set, dashed curves) as well as the global OMP parameter set of McFadden and Satchler [35] (dotted curves).

V. CONCLUSIONS

The analysis of the α-particle elastic scattering on A$\sim$100 nuclei at energies below 32 MeV has been performed using the semi-microscopic DF approach. The energy-dependent phenomenological OMP imaginary part, which was obtained in this case, making use also of the dispersive correction to the DF real potential, has been then used for a completely phenomenological analysis of the same data basis. Altogether the results of this analysis support the concept to deduce the phenomenological part for the potentials to describe alpha-particle scattering data by the use of microscopic calculations. The number of free parameters are decreased by using the real DF potential and by adjusting only the imaginary OMP part parameters. In the next step we adjusted only the parameters of the real phenomenological potential of Woods-Saxon shape while the imaginary components remained unchanged. The last step of fine tuning has been performed in order to provide finally a regional parameter set to be easily used in further analyses or predictions. We have thus found that our regional potential is able to describe appropriately even nuclear absorption within the particular case of Wit *et al.* data [20] at 23 MeV. From systematics of α-particle scattering it has been known that the potentials must be deep [38,39], approximately 150 MeV at small distances. At our energies the deep potential is important for the inner turning point contributions needed to describe the large angle scattering. This is also the result of the present DF analysis.

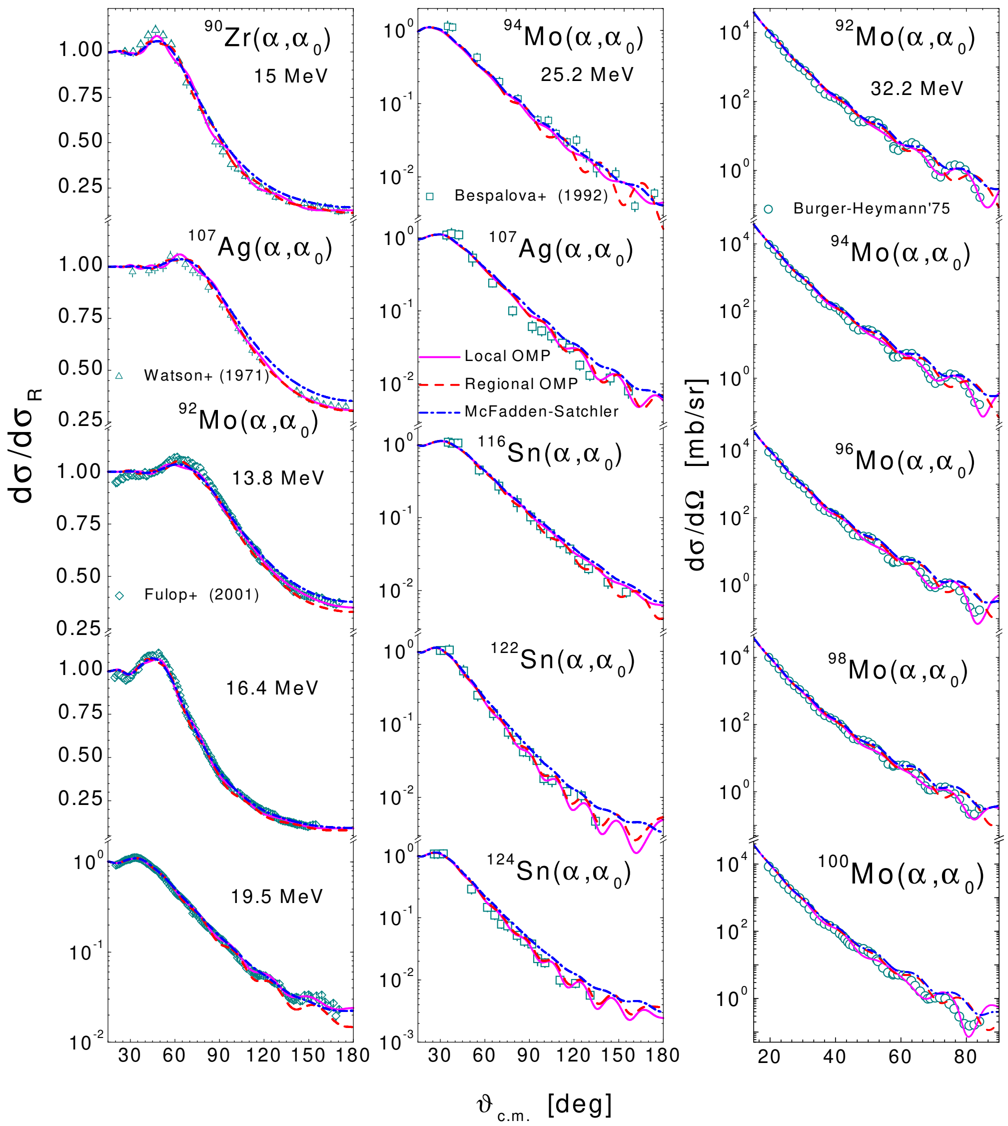

FIG. 5. The same as in Fig. 2 for angular distributions of the elastic scattering of α-particles, by using the same phenomenological OMP parameter sets as in Fig. 4.

The α-particle energy range of this regional OMP is below 40 MeV. It can be used and checked in the analysis of the α-induced or (n,α) reaction cross sections which were not taken into account in this work in order to avoid the discussion of the rest of the statistical-model parameters as well as the effects expected for the α-particles emitted from compound reactions, e.g. (n,α), due to excited residual nuclei. Further work will concern the whole mass range as well as the energies between 40 and 80 MeV.

ACKNOWLEDGMENTS

One of the authors (M.A.) acknowledges the hospitality and support of the Hahn-Meitner-Institut, Berlin, the EC/JRC Institute for Reference Materials and Measurements, Geel, and the Abdus Salam International Centre for Theoretical Physics, Trieste. This work was supported in part by the Contract No. ERB-5005-CT-990101 of Association between EURATOM and MEC-Bucharest, and the IAEA-Vienna Research Contract No. 12422.

[1] S. Goriely, J. Nucl. Sci. Technol. Suppl. 2 (2002) 536.
[2] P. Obložinský (Ed.), Development of Reference Input Parameter Library (RIPL) for Nuclear Model Calculations of Nuclear Data, Report IAEA-TECDOC-1034, IAEA, Vienna, 1998; http://www-nds.iaea.or.at/ripl/.
[3] Dao T. Khoa, Phys. Rev. C 63 (2001) 034007.
[4] Zs. Fülöp, Gy. Gyürky, Z. Máté, E. Somorjai, L.Zolnai, D. Galaviz, M. Babilon, P. Mohr, A. Zilges, T. Rauscher, R. Oberhummer, G. Staudt, Phys. Rev. C 64 (2001) 065805.
[5] P. Demetriou, C. Grama, S. Goriely, Nucl. Phys. A707 (2002) 253.
[6] M. Avrigeanu, W. von Oertzen, A.J.M. Plompen, V. Avrigeanu, Nucl. Phys. A 723 (2003) 104.
[7] Dao T. Khoa, G.R. Satchler, Nucl. Phys. A668 (2000) 3.
[8] Dao T. Khoa, W. von Oertzen, Phys. Lett. B 304 (1993) 8; B 342 (1995) 6;
Dao T. Khoa, W. von Oertzen, H.G. Bohlen, Phys. Rev. C 49 (1994) 1652;
Dao T. Khoa, W. von Oertzen, A.A. Ogloblin, Nucl. Phys. A602 (1996) 98;
D.T. Khoa, G.R. Satchler, W. von Oertzen, Phys. Rev. C 56 (1997) 954.
[9] M. Avrigeanu, A.N. Antonov, H. Lenske, I. Şteţcu, Nucl. Phys. A693 (2001) 616;
I.V. Krouglov, M. Avrigeanu, W. von Oertzen, Eur. Phys. J. A 12 (2001) 399;
M. Avrigeanu, G.S. Anagnostatos, A.N. Antonov, J. Giapitzakis, Phys. Rev. C 62 (2000) 017001.
[10] G. Bertsch, J. Borysowicz, H. McManus, W.G. Love, Nucl. Phys. A284 (1977) 399.
[11] N. Anantaraman, H. Toki, G. Bertsch, Nucl. Phys. A398 (1983) 279.
[12] F.E. Steigert, M.B. Samson, Phys. Rev. 92 (1953) 660.
[13] T.A. Tombrello, L.S. Senhouse, Phys. Rev. 129 (1963) 2252.
[14] W.S. Chien, R.E. Brown, Phys. Rev. C 10 (1974) 1767.
[15] D. Baye, L.Desorgher, D. Guillain, D. Herschkowitz, Phys. Rev. C 54 (1996) 2563.
[16] J.W. Negele, Phys. Rev. C 1 (1970) 1260.
[17] J.W. Lightbody, Jr., S. Penner, S.P. Fivozinsky, P.L. Hallowell, H. Crannell, Phys. Rev. C 14 (1976) 952.
[18] M. El-Azab Farid, G.R. Satchler, Nucl. Phys. A438 (1985) 525.
[19] B.D. Watson, D. Robson, D.D. Tolbert, R.H. Davis, Phys. Rev. C 4 (1971) 2240.
[20] M. Wit, J. Schiele, K.A. Eberhard, J.P. Schiffer, Phys. Rev. C 12 (1975) 1447.
[21] O.V. Bespalova, E.A. Romanovskij, N.G. Gorjaga, Nguen Mak Kha, B.S. Galakhmatova, Luaj Morzena Rafu, S.I. Fedoseev, Dang Lam, Anis Belal, Yad. Fiz. 56 (1992) 113.
[22] S.J. Burger, G. Heymann, Nucl. Phys. A243 (1975) 461.
[23] O. Bersillon, Centre d'Etudes de Bruyeres-le-Chatel, Note CEA-N-2227, 1992.
[24] M. Nolte, H. Machner, J. Bojowald, Phys. Rev. C 36 (1987) 1312.
[25] V. Avrigeanu, P.E. Hodgson, M. Avrigeanu, Phys. Rev. C 49 (1994) 2136.
[26] D.M. Brink, N. Takigawa, Nucl. Phys. A279 (1977) 159.
[27] H. Abele, G. Staudt, Phys. Rev. C 47 (1993) 742.
[28] A. Ingemarsson, J. Nyberg, P.U. Renberg, O. Sundberg, R.F. Calrson, A.J. Cox, A. Auce, R. Johansson, G. Tibell, Dao T. Khoa, R.E. Warner, Nucl. Phys. A676 (2000) 3.
[29] C. Mahaux, H. Ngo, G.R. Satchler, Nucl. Phys. A449 (1986) 354.
[30] C. Mahaux, H. Ngo, G.R. Satchler, Nucl. Phys. A456 (1986) 134.
[31] G.R. Satchler, Phys. Rep. 199 (1991) 147.
[32] F. Michel, G. Reidemeister, S. Ohkubo, Phys. Rev. C 61 (2000) 041601(R).
[33] J. Albinsky, F. Michel, Phys. Rev. C 25 (1982) 213.
[34] F. Michel, J. Albinski, P. Belery, Th. Delbar, Gh. Gregoire, B. Tasiaux, G.Reidemeister, Phys. Rev. C 28 (1983) 1904.
[35] L. McFadden, G.R. Satchler, Nucl. Phys. A84 (1966) 177.
[36] P. Mohr, T. Rauscher, R. Oberhummer, Z. Máté, Zs. Fülöp, E. Somorjai, M. Jaeger, G. Staudt, Phys. Rev. C 55 (1997) 1523.
[37] P. Mohr, Phys. Rev. C 61 (2000) 045802.
[38] G.R. Satchler, Direct Nuclear Reactions, Oxford University Press, Oxford, 1983, p. 490.
[39] F. Michel, S. Ohkubo, G. Reidmeister, Prog. Theor. Phys. Suppl. 132 (1998) 7.